Running title: Deep brain photoreceptors in birds

Title: Functional inhibition of deep brain non-visual opsins facilitates acute long day induction of reproductive recrudescence in male Japanese quail.

Authors: Jonathan H. Pérez*[1], Elisabetta Tolla[2], Valerie R. Bishop[3], Russell G. Foster[4], Stuart N. Peirson[4], Ian C. Dunn[3], Simone L. Meddle[3], Tyler J. Stevenson[2].

Affiliation: 1. Biology Department, The University of South Alabama, Mobile Alabama, 36688, USA.
2. Institute of Biodiversity, Animal Health and Comparative Medicine, University of Glasgow, Glasgow G61 1QH, Scotland.
3. The Roslin Institute, The Royal (Dick) School of Veterinary Studies, University of Edinburgh, Midlothian EH25 9RG, Scotland.
4. Sir Jules Thorn Sleep and Circadian Neuroscience Institute (SCNi) and Nuffield Laboratory of Ophthalmology, Nuffield Department of Clinical Neurosciences, Dorothy Crowfoot Hodgkin Building, University of Oxford, South Parks Road, Oxford OX1 3QU.

*Corresponding author
Biology Department
The University of South Alabama
Mobile, AL 36688
5871 USA Dr
Email: jhperez@southalabama.edu
Phone: 251-460-6331

Disclaimer: The authors have nothing to disclose.

Key words: photoreceptor, VA opsin, neuropsin, OPN5, seasonality, reproduction, RNA interference, viral vector

Highlights

- VA opsin and neuropsin RNAi silencing impact photoinduced activation of the reproductive axis in quail
- Effects of RNAi silencing of VA opsin and Opn5 variably impact reproductive axis activity
- Non-visual opsin photoreceptors appear to exert their effect at multiple points in the regulation of the reproductive axis.

Abstract

For nearly a century, we have known that brain photoreceptors regulate avian seasonal biology. Two photopigments, vertebrate ancient opsin (VA) and neuropsin (OPN5), provide a possible molecular substrate for this photoreceptor pathways. VA fulfills many criteria for providing light input to the reproductive response, but a functional link has yet to be demonstrated. This study examined the role of VA and OPN5 in the avian photoperiodic response of Japanese quail (*Coturnix japonica*). Non-breeding male quail were housed under short days (6L:18D) and received an intracerebroventricular infusion of adeno-associated viral vectors with shRNAi that selectively inhibited either VA or OPN5. An empty viral vector acted as a control. Quail were then photostimulated (16L:8D) to stimulate gonadal growth. Two long days significantly increased pituitary thyrotrophin-stimulating hormone β-subunit (*TSHβ)* and luteinizing hormone β-subunit (*LHβ)* mRNA of VA shRNAi treated quail compared to controls. Furthermore, at one week there was a significant increase, compared to controls, in both hypothalamic gonadotrophin releasing hormone-I (*GnRH-I*) mRNA and paired testicular mass in VA shRNAi birds. Opn5 shRNAi facilitated the photoinduced increase in *TSHβ* mRNA at 2 days, but no other differences were identified compared to controls. Contrary to our expectations, the silencing of deep brain photoreceptors enhances the response of the reproductive axis to photostimulation rather than preventing it. In addition, we show that VA opsin plays a dominant role in the light-dependent neuroendocrine control of seasonal reproduction in birds. Together our findings suggest the photoperiodic response involves at least twoAfter 7 days of photostimulation of VA opsin either directly co-expressed in GnRH-I neurons or indirectly (via disinhibition from VA neurons) resulted in higher GnRH expression and increased LHβ and FSHβ expression photoreceptor types and populations working together with VA opsin playing a dominant role.

Introduction

Annual changes in photoperiod, are the primary predictive cue regulating seasonal reproduction in many vertebrates (Dawson et al., 2001; Rowan, 1925). The photoperiodic response is a well characterized cascade of neuroendocrine changes that transition birds from a short day (SD) non-breeding to a long day (LD) reproductive state (Follett and Pearce-Kelly, 1991; MacDougall-Shackleton et al., 2009). Exposure to a single day of photoperiod exceeding 13 hours of light stimulates thyrotrophs in the pars tuberalis to release *TSHβ*, inducing a reciprocal switch in deiodinase gene expression in the MBH (Nakao et al., 2008). Continued long-term LD exposure maintains high GnRH-I synthesis in the preoptic area (POA) and permits GnRH-I release, to stimulate luteinizing hormone (LH) and follicle-stimulating hormone (FSH) release from the anterior pituitary gland.

In mammals, a discrete population of retinal ganglion cells, expressing the non-visual photoreceptor melanopsin (OPN4), are critical for transduction of seasonal light information (Foster et al., 2020; Hankins et al., 2008). However, in most non-mammalian species, light-driven changes in seasonal physiology occur via extra-retinal photoreceptors (Menaker et al., 1970; Menaker and Keatts, 1968; Pérez et al., 2019). Targeted illumination studies have localized the photoreceptors for avian reproduction to the medial basal hypothalamus (MBH) (Benoit and Ott, 1944; Oliver and Baylé, 1975). The action spectrum (λ_{max}) for reproductive photostimulation in Japanese quail (*Coturnix japonica*) established the involvement of an opsin/vitamin-A based photopigment with a maximum spectral response of ~492 nm (Foster et al., 1985; Foster and Follett, 1985). To date, three photoreceptor opsins have been characterized and localized within the hypothalamus of birds: vertebrate ancient opsin (VA; Halford et al., 2009), neuropsin (OPN5; Nakane et al., 2014) and melanopsin (OPN4; Chaurasia et al., 2005).

VA is expressed in the preoptic area (POA) and mediobasal regions of the hypothalamus (Halford et al., 2009). Crucially, VA cells exhibit an absorption spectrum closely matching the reproduction spectra maximum for reproductive physiology (~490nm; Davies et al., 2012) and are co-localize with gonadotropin-releasing hormone I (GnRH-I) expressing cells (Halford et al., 2009) providing a link between light detection and activation of the reproductive axis (García-Fernández et al., 2015). However, a functional role for VA in the photoperiodic response has yet to be demonstrated. OPN4 is expressed in the pre-mammillary nucleus of turkeys (*Meleagris gallopavo*) (Kang et al., 2010), with very low OPN4 expression recently reported in the quail infundibular hypothalamic region (Nakane et al., 2019). However, the lack of strong mediobasal localization suggests that OPN4 is not likely to be the primary photoreceptor for reproduction in birds (Peirson and Foster, 2006). Conversely, histological analyses have demonstrated that OPN5-expressing cells are localized to the periventricular organ (PVO) within the mediobasal hypothalamus. OPN5 cells project towards the pars tuberalis, a region involved in coordinating GnRH-I release (Nakane et al., 2014), yet OPN5 has an absorption spectrum (420 nm); considerably lower than the reported maxima of ~492nm for photoperiodic induction. Functional studies have shown that RNA inhibition of OPN5 alters thyrotrophin-stimulated hormone β-subunit (*TSHβ*), a key gene in the photostimulation of reproduction, expression in canaries (*Serinus canaria*) (Stevenson and Ball, 2012), red-headed bunting (*Emberiza bruniceps*) (Majumdar et al., 2014) and Japanese quail (Nakane et al., 2014). But OPN5 has not been linked directly to other upstream components of the reproductive axis.

The three main components of the avian reproductive response are: i) deep brain photoreceptor(s), ii) a circadian clock (Follett and Sharp, 1969) and iii) GnRH-I synthesis and secretion (Stevenson et al., 2012). To date, only OPN5 has been functionally implicated in the

acute photoinduced regulation of *TSHβ.* No study has examined the functional role of VA, nor the long-term role of any photoreceptor. To address this deficit in knowledge, the current study aimed to establish any functional roles that VA and OPN5 opsins may play in the photoperiodic regulation of reproduction in the Japanese quail. Short-hairpin RNA (shRNA) constructs packaged in adeno-associated virus (AAV) were used to test the hypothesis that VA and/or OPN5 are necessary for i) the short-term photoinduction of *TSHβ*, *GnRH-I*, *LHβ-subunit* and *FSHβ-subunit* (*FSHβ)* mRNA expression, and ii) are involved in the development and maintenance of photoinduced reproduction.

Materials and Methods

Ethical approvals

Animal procedures were approved by the Roslin Institute Animal Ethics and Welfare Review Board at the University of Edinburgh and were performed under Home Office approval (PPL P61FA9171). The experiments were designed in accordance with the Animal Research Reporting of In Vivo Experiments (ARRIVE) guidelines and National Centre for the Replacement, Refinement and Reduction of Animals in Research.

Adeno-associated viral vector, shRNA design and cellular expression

Custom adeno-associated virus serotype 2 vectors containing shRNA templates targeting either OPN5 (*vOPN5*) or VA (*vVA*) were produced by Virovek (Hayward, CA). shRNAi contained a hair-pin loop insert (TCAAGAG); both *vVA* and *vOPN5* targeted exon 4 (S1 Table and Fig. 1A). To identify any potential off-target effects, Blastn search was conducted, no sequences with high homology (>90%) were identified against the shRNAi. The low homology

aligned sequences identified by Blastn are not associated with regulation of the photoperiodic response and nor expressed in the mediobasal hypothalamus, giving confidence that RNA interference induced by the shRNAi constructs are highly specific for VA and OPN5.

shRNAi were expressed under a constituently active CMV promoter in an expression cassette, which also contains green fluorescence protein (GFP) to facilitate infected cell identification (Fig.1B). The CMV expression cassette was selected based on pilot tests using primary cell culture to confirm the capability of AAV2 to successfully transfect and be expressed in quail nervous tissue (Fig. 1).

Animals

All studies used adult (>12-week-old) male Japanese quail (*Coturnix japonica*) hatched and reared at the National Avian Research Facility, University of Edinburgh, Scotland, UK until at least 3 months of age. Birds were provided food and water *ad libitum*. Following rearing, birds were transferred to short days (6L:18D; Lights on at 07:00) for at least 8 weeks to ensure all birds were in a photosensitive, non-breeding condition (Follett and Pearce-Kelly, 1991).

Pilot testing of AAV2 vectors

To determine suitability of the AAV2 vector construct, primary cell culture testing using neural explants from embryonic quail were conducted. The basal portion of a day 10 quail embryo brain (10 days of incubation; quail hatch at E18) was explanted and homogenized to generate a primary cell culture for testing. Explants were transferred to ice cold phosphate buffered saline (PBS) and then cultured in sterile 24 well culture plates with 500 µl of incubation media overnight at 37oC with 5% CO2. Incubation media contained Dulbecco's Modified Eagle

Medium (DMEM; Fisher Scientific) base with 1% Penstrep and 10% fetal bovine serum (Fisher Scientific). Following overnight incubation 400 ul of incubation media was removed and replaced with 600 µl of fresh incubation media containing 4 µl, 2 µl, 1 µl or 0.5 µl of Virovek's AAV2-CMV vector containing only GFP (Vector Labs, Hayward CA.; 2-2.5E+13 vg/100 ul). Incubation media was refreshed daily and explants were cultured for five days prior to fluorescent imaging. GFP presence or absence was determined by fluorescence microscopy (Zeiss Axiovert 25 and 100 fluorescent microscopes with Axiocam 503c cameras running Zeiss Zen software; Figure S1C). Both 4 µl and 2 µl doses of vector produced strong detectable signal distinctly localized to individual cells, indicating reliable transfection.

Stereotaxic intracerebroventricular injection of shRNA-AAV2 vectors

AAV2 vectors were delivered via stereotaxic intracerebroventricular (ICV) injection into the third ventricle (3V) of the medial basal hypothalamus (MBH). Injection coordinates were refined from estimates taken from the adult quail brain atlas (Baylé et al., 1974) using test injections of India ink into fresh quail cadavers. Following test injections, brains were removed, frozen on dry ice and coronally sectioned on a cryostat at 50 µM. Sections were mounted to glass microscope slides for rapid visualization via light microscopy. This process was repeated iteratively to optimize the anatomical localization of injections directly into the MBH. The final coordinates used were determined with respect to the bursa as X = 0.0 mm, y = 3.8 mm, and z = -6.3 mm then pulled up to -6.0 mm for injection.

All experimental ICV injections were performed following standard protocols developed in consultation with the Named Veterinary Surgeons using aseptic technique. Birds were

anesthetized with isoflurane (4-5%) administered by facemask with 1.5 L/min of O_2, following induction of anesthesia Isoflurane was reduced to ~2%, monitored and adjusted continually by the anesthetist to maintain desired anesthetic depth. Animals then received subcutaneous injections of meloxicam (0.5 mg/kg) and butorphanol (1.5 mg/kg) as analgesia prior to positioning in the stereotaxic frame (Kopf Instruments). Feathers were plucked and the surgical site cleaned with Hibiscrub. A small ~1 cm incision was made by scalpel to expose the skull. The tip of the injection syringe was aligned to the bursa and zeroed then moved to the injection coordinates and a small mark placed with a pencil prior to clearing the syringe. A dental ball mill drill bit (size #4; WPI) was used to drill a small hole (~ 1-2 mm in diameter) though the skull. The syringe was then realigned and coordinates verified prior to insertion of the needle to target coordinates. A 10 ul Hamilton syringe fitted with a sterilized 28-gauge microfillers (WPI MF28G-5; 97mm, 0.35mm OD, 0.25mm ID) trimmed to half-length were used for injections. Birds were injected with 1 μL of AAV2 at ~2.34E+13 vg/ml containing: blank cassette shRNAi (control, CV), shRNAi vOPN5 or shRNAi vVA. The surgical incision was closed either by veterinary adhesive (VetBond 3M) or sutures. Animals recovered in an isolated box before transfer to a communal recovery pen, equipped with food, water and a heat lamp. The photoperiod was lengthened by one-hour (7L:17D) to facilitate recovery.

Study 1: The effect of acute photoinduction and shRNAi on the hypothalamic-pituitary-gonadal axis

To establish a non-breeding baseline of target gene expression, as well as determine any direct effects of the AAV2 vector, a subset of birds (n = 5) were injected with the CV vector whilst kept on SD (7L:17D) for 2 weeks and then culled. Birds were closely monitored during

this period for signs of any adverse effects. All birds remained healthy and the main experiment commenced.

To determine the effects of opsin silencing on the initial photoinduction of the reproductive axis birds were injected with CV (n = 5), *vOPN5* (n = 5) or *vVA* (n = 8) held on short days SD (7L:17D; lights on 07:00) for 2 weeks and then transferred to 16L:8D for 2 days or 7 days (CV n= 6, *vOPN5* n = 9, *vVA* n= 7) prior to collection. Blood samples ($\leq$ 250 µl) were collected by venipuncture of the wing vein using a 26-gauge needle and collected from the surface using heparinized microcapillary tubes. Blood was collected from all birds 2 days prior to photostimulation and then again at cull (2 or 7 days). In total across treatments and time points 45 quail were used in the experiment (CV n=16, vOPN5 n=14, vVA n=15). Plasma was separated by centrifuging the microcapillary tubes at 10,000 g for 5 minutes, aspirated and then stored at -20°C until assay for testosterone. Birds were euthanized by cervical dislocation followed by rapid decapitation between the hours of 10:00 and 12:00. This early phase of the light-dark cycle was selected due the increased levels of gonadotropins identified previously (Meddle and Follett, 1997, 1995). Brain and pituitary stalk tissues were rapidly dissected and fresh frozen on dry ice. Both testes were dissected and weighed on an analytical balance (Sartoris model A200S) to the nearest 0.1g. All tissues were stored at -80°C.

Study 2: The effect of chronic photostimulation and shRNAi on the photoperiodic response

To determine the effects of long-term opsin silencing a second study was conduct by transferring birds from SD to LD for 28 days, a period well-established to stimulate maximal gonadal growth (Follett and Pearce-Kelly, 1991). Birds were pseudo-randomly administered with ICV shRNAi containing either i) CV (n= 8), or treatment groups that consisted of ii) *vVA* opsin

shRNAi (n= 9), or iii) *vOPN5* shRNAi (n= 9), then kept on a photoperiod of 7L:17D for 2 weeks and then photostimulated (16L:8D). Blood samples (≤ 250 µl) were collected as described above 2 days pre-photostimulation and then at 7, and 28 days following photostimulation. Blood was centrifuged and plasma aspirated as above and stored at -20°C until assay. Tissues were dissected and stored as described above.

Brain sectioning and AAV GFP histological localization

Brains from the second study were coronally sectioned at 30 µm, mounted onto polysine slides (Fisher 10219280) and cover slipped with VECTASHIELD Antifade Mounting Media with DAPI (Vector Labs, Burligame, CA USA). Slides were examined under fluorescence microscopy to confirm localization of GFP signal to the MBH (Fig. 1). Birds where injections were found to be off target, or there was no sign of injection were excluded from subsequent analyses (see below).

Western Blot assays of hypothalamic extracts for VA and OPN5

Polyclonal antibodies against VA and OPN5 were custom made by Cambridge Research Biochemicals, Inc. (see Supplemental Table 3 for target sequences) in rabbit hosts with sub-fractions of collected sera purified via affinity chromatography. Antibody sequence target were selected based on previously published specificity for VA (Halford et al., 2009) and OPN5 (Nakane et al., 2010). BLASTp analyses confirmed that the OPN5 sequence has 100% sequence homology with the predicted OPN5 target and non-specific hits were <80% homology with

<80% coverage. For VA there was 100% identity and 100% coverage of the antibody sequence for the Japanese quail sequence, confirming the high homology. Furthermore, there was low non-specificity for off-target sequences with <80% identity and <80% coverage.

To confirm reduced VA and OPN5 protein expression, western blots were conducted on hypothalamic protein extracts. The hypothalami were dissected (as described above) and homogenized in 700 µl of 100 mM Tris-HCL buffer with 4% w/v SDS and protease inhibitors (Halt™ Protease Inhibitor Cocktail, EDTA-free, Thermo Fisher Scientific). Samples were then centrifuged at 20,000 x g for 20 minutes at 4°C. Supernatant was collected and stored at -80°C. Total protein concentration for all samples was determined using 1 µl of supernatant using a BCA Protein Assay (Pierce™ BCA Protein Assay Kit) per manufacturer's instructions. Supernatant volume for use in western blots was then standardized to add 10 µg of protein to each well by diluting with water. 20 µl of diluted sample was combined with 10 µl of LDS buffer (NuPAGE™ LDS Sample Buffer, Thermo Fisher Scientific) then incubated at 98°C for 2 minutes prior to loading. Samples were loaded onto 4-12% Bis-Tris pre-cast gels (NuPAGE™, Thermo Fisher Scientific), 10 µl per sample and were loaded onto two separate gels that were run in parallel in the same gel tank. Treatment groups were spread across gels. Gels were run at 90V or 5 minutes to ensure even entry of samples into the gel, then at 175V for 1 hour. One duplicate gel was then immediately incubated in 40 ml of OptiBlue protein stain for 1 hour, to quantify total protein loading, on an orbital shaker. The second gel was then processed for western blot transfer. Protein was transferred to a PDVF membrane (iBlot™ Transfer Stacks, PVDF, regular size, Thermo Fisher Scientific) using the iBlot 2 system. Membranes were then washed in 1X PBS 5 times for 5 minutes before being blocked for 30 minutes in Odyssey blocking buffer in 50 ml falcon tubes. Blocking buffer was discarded and replaced with 5 ml of

primary antibody solution (5 ml Odyssey buffer, 1 AB, 0.1% Tween 20). Following primary antibody incubation, samples were rinsed in PBS 6 times for 5 minutes. Incubation with secondary antibody was performed using IRDye 680RD Goat Anti-Rabbit antibody (LI-COR) at 1:10,000 in 5 ml Odyssey Blocking Buffer with 0.1% Tween 20 before being incubated in secondary antibody for 90 minutes at room temperature. Membranes were then rinsed with PBS 6 times for 5 minutes prior to imaging. Membranes were imaged on a LI-COR Odyssey imager using Image Studio software (Image Studio™ LI-COR). Western blots were imaged at 3.5 intensity, medium image quality at 169 µm resolution. Total protein gels were rinsed in distilled water and then imaged on the 700 nm channel at lowest image quality, Intensity 3, 169 µm resolution.

Enzyme-linked immunosorbent assay (ELISA) for testosterone

To measure plasma testosterone levels, the Parameter™ Testosterone Assay (R&D Systems, Bio-Techne) was used according to manufacturer's instructions. Samples were assayed in duplicate using 50 µl plasma and absorbance was measured at 450 nm and 570 nm using a microplate reader (LT-4500, Labtech). For each well, the value from 570 nm was subtracted from the value for 450 nm to obtain a normalized fluorescent measurement. The sensitivity of the assay ranged from 0.012-0.041 µg/ml. Cross-reactivity of the assay was <0.1% for androsterone, estradiol, prednisolone and progesterone. Two assays were conducted, the intra-assay coefficient of variation was 7.7% and 9.4%. The inter-assay coefficient of variation was 13%.

RNA isolation and cDNA synthesis

Hypothalami were dissected from the first study using well characterized neuroanatomical landmarks (Baylé et al., 1974; Pérez et al., 2020). Hypothalami were then homogenized in 700 µl of 100 mM Tris-HCL buffer with 4% w/v SDS and protease inhibitors (Halt™ Protease Inhibitor Cocktail, EDTA-free, Thermo Fisher Scientific). Homogenized samples were then centrifuged to pellet debris and the supernatant was then transferred to clean microcentrifuge tubes for protein analysis (S1 File). Hypothalamic pellets and pituitary glands were homogenized using 1 ml of TRIzol (Thermo Fisher Scientific) using a Kinematica Polytron PT1200E handheld homogenizer (Thermo Fisher scientific). Following a 5minute room temperature incubation, 200 µl of chloroform was added to each sample and vortexed to mix. Samples were then incubated for 3 minutes at room temperature, then centrifuged at 12,000 g for 15 minutes at 4°C. The upper aqueous phase was pipetted into a fresh microcentrifuge tube. 500 µl of isopropanol was added and incubated for 10 minutes. Tubes were centrifuged again at 12,000 g for 15 minutes at 4°C. Supernatant was discarded and the pellet re-suspended in 1 ml of 75% ethanol. Samples were centrifuged at 7,500 g for 5 minutes at 4°C and supernatant discarded. The remaining pellet containing the RNA was re-suspended in 30 µl of RNase-free water. Nucleic acid quality (260/280) and concentration was determined by Nanodrop (Thermo Fisher Scientific). 2 µg of RNA was reverse transcribed using a Precision nanoScript2 Reverse Transcription kit (Primerdesign Ltd) following the manufacturer's instructions and cDNA was stored at -20°C until quantification.

Real-time quantitative PCR (qPCR)

qPCRs were performed on a Stratagene Mx3000 Real Time PCR machine in 20 µl reactions. For each well, the qPCR mix consisted of 5 µl cDNA template, 10 µl SYBR green

328 (Primerdesign Ltd), 0.5 µl (300nM) forward primer, 0.5 µl (300nM) reverse primer and 4 µl
329 RNase-free H2O. Samples were run in duplicate in a 96-well plate format under the following
330 conditions: i) denaturing at 95°C for 5 min., then 39 cycles of ii) 95°C for 10 s, iii) 30 s at
331 annealing temperature dependent on primer (See Table 2), and finally iv) an extension step of
332 72°C for 30 s. Melt curves were analyzed to ensure the specificity of each reaction. PCR
333 Miner (Zhao and Fernald, 2005) was used to determine reaction efficiencies and
334 quantification cycle (Ct). Fold expression was measured in relation to
335 the average Ct for two reference genes (*GAPDH* and *βACTIN*) and calculated using 2-
336 (ΔΔCt). The average Ct obtained from short day CV treatment group was used as the second
337 delta value in order to identify photoinduced changes in transcript levels.
338

339 # Exclusion criteria

340 Some quail were excluded from statistical analyses based on both a priori exclusion
341 criteria and based on outlier testing during statistical analysis. For the first study, one short day
342 control bird, two CV and 3 *vOPN5* shRNAi treated birds were removed because testicular mass
343 values were indicative of breaking the non-breeding state (i.e. 1.4 - 3.2g) while still on short
344 days. Opsin silencing was confirmed by both Western Blot and qPCR to confirm high efficiency
345 of AAV2 vector delivery to MBH (S1G and S1H Fig). Two *vOPN5* and two *vVA* treated birds
346 were excluded from analyses due to mRNA expression values being similar to control treated
347 birds, as a consequence of off-target viral injections. One *vOPN5* bird was excluded from the
348 western blot validations because of a technical error in gel loading. In the second study birds
349 were screened for inclusion by presence of GFP signal in the MBH, taking advantage of the

AAV2 vector's GFP expression (independent of shRNA. One CV and one *vOPN5* were excluded based on lack of GFP expression in the MBH. Raw data and R code are available in S2 File.

Statistical analyses

All statistical analyses were conducted in R v 4.0.2 (R Core Development Team, 2020) using the following packages: car (Fox and Weisberg, 2019), emmeans (Lenth et al., 2018), grid (Murrell, 2005), ggthemes (Arnold, 2017), ggpubr (Kassambara, 2019), and tidyverse (Wickham et al., 2019). Paired testes mass was analyzed by linear model. Model assumptions were checked by graphic visualization of residual outputs using the plot() function to confirm model fit. Initially, RNA expression data failed to fit linear model assumptions even when log transformed, therefore, these data were subsequently analyzed by generalized linear model using a gamma distribution with a log link. Model fit was checked via visualization of model residuals; use of gamma models improved model fit based on AIC. Main effects within the model were assessed using a Likelihood Ratio Test.

Results

Long day stimulation of testicular growth

In order to determine the long-term functional role of VA and OPN5, SD photosensitive birds received a single intracerebroventricular (ICV) injection of shRNAi constructs targeting VA (*vVA*), OPN5 (*vOPN5*), or empty cassette (CV) and then after a two-week recovery, were exposed to stimulatory photoperiods for either 2, 7 or 28 days. Testes mass was significantly heavier 7 days post photostimulation in all birds (Fig 2A; $F_{1,37}$=14.69, p<0.001, partial η^2 =

372 0.562). There was no detectable interaction effect for days post photostimulation and ICV
373 injection ($F_{2,37}$=2.66, p=0.083, partial η^2 = 0.126). However, based on the loss of statistical power
374 (<0.8) due to imbalance in sample sizes across treatments, and following visual inspection of
375 plotted data, opted to investigate photoinduced increases in testes mass at 2, 7, and 28 days post-
376 photostimulation separately as well.
377
378 We found that 2 days following photostimulation there was no effect of shRNAi
379 silencing on testes mass ($F_{2,13}$=0.35, p=0.713, partial η^2 = 0.05). After 7 days of
380 photostimulation, shRNAi silencing resulted in a significant increase in testes mass ($F_{2,19}$=4.31,
381 p=0.029, partial η^2 = 0.312), with *vVA* injected birds having heavier testes compared to control
382 (CV) birds (t=-2.78, p=0.031, Cohen's d = 1.50) suggesting that *vVA* treatment facilitated the
383 photoperiod induced growth of testes. There was no difference detected at 7 days between
384 *vOPN5* and CV birds (t=-0.80, p=0.706, Cohen's d = 0.49) not *vVA* and *vOPN5* birds (t=-2.23, p
385 = 0.092, Cohen's d = 1.03). There was no significant difference in testes mass between birds that
386 received shRNAi against OPN5 or VA for 28 days compared to CV (Fig 2B; $F_{2,23}$=0.28,
387 p=0.761, partial η^2 = 0.024). These data indicate that shRNAi of VA facilitated the long day
388 photoinduced transition (i.e. day 7) to a fully photostimulated reproductive state, accelerating
389 gonadal growth, which was complete in all birds by 28 days regardless of treatment.
390

391 # Long days increased plasma testosterone concentrations

392 As testosterone is the predominant hormone produced by the testes, we sought to identify
393 whether circulating concentrations would parallel long day induced increases in testes mass.
394 There was no significant effect of treatment on plasma testosterone following 2 days of LD (Fig

2C; LR $\chi2$=0.81, p=0.667, partial η^2 = -0.933) nor an interaction of shRNAi injection and days post-photostimulation (LR $\chi2$=0.64, p=0.726, partial η^2 = 0.438). Testosterone significantly increased from 2 to 7 days post-photoinduction (LR $\chi2$=104.70, p<0.001, partial η^2 = 0.938). Chronic silencing had no effect on plasma testosterone after 28 days (LR $\chi2$=0.52, p=0.77, partial η^2 = 0.941). The lack of an effect of shRNAi on plasma testosterone concentrations at 28 days suggests that VA and OPN5 do not regulate short-term, daily rhythms in reproductive physiology and instead, confirms their role in the long-term photoperiodic response.

Long days and shRNAi increased hypothalamic GnRH-I expression

Next, we sought to determine the neuroendocrine mechanisms underlying the shRNAi induced increase in testicular mass. Using quantitative PCR (qPCR) we examined hypothalamic *GnRH-I* and *GnIH* expression. There was a significant interaction for hypothalamic *GnRH-I* expression between injection and days post photoinduction (Fig 3A; LR χ^2=16.70, p<0.001, partial η^2 = 0.996) as well as a significant main effect of ICV injection (LR χ^2=10.59, p=0.005, partial η^2 = 0.929). Post hoc testing using Student's T distribution via the summary.glm() function indicated a significant increase in hypothalamic *GnRH-I* expression in *vVA* birds at 7 days when compared to CV (t_{18}=2.25, p=0.037, Cohen's d = 1.121), no other differences were detected. Conversely, *GnIH* expression did not change following either 2 or 7 LD (Fig 3B; LR $\chi2$=2.81, p<0.094, partial η^2 = 0.261). There was also no effect of ICV injection (LR $\chi2$=0.29, p=0.867, partial η^2 = 0.232) nor an interaction between injection and days post photoinduction (Fig 3D; LR $\chi2$=0.99, p=0.610, partial η^2 = 0.853). Taken together, these data indicate that VA either directly (Halford et al., 2009) or indirectly is involved in regulating the photoperiod induced increase in testicular mass via the master neuropeptide for reproduction, GnRH-I.

Long days regulate anterior pituitary secretagogue expression

Next, we investigated whether gonadotroph release from the pituitary gland was regulated by shRNAi of VA and OPN5. Using qPCR, we assessed the photoperiod induced change in *LHβ*, *FSHβ*, and *TSHβ* expression in birds after 2, 7 and 28 days. There were no significant effects of ICV injection (LR $\chi2 = 0.43$, $p = 0.807$, partial $\eta^2 < 0.001$), following LD transfer, nor any interaction between injection and days of photostimulation (LR $\chi2 = 1.55$, $p = 0.460$, partial $\eta^2 = 0.447$). As the findings indicated increased variation in *LHβ* expression at 2 LD, the effect of shRNAi on 2- and 7 LD were examined separately. There was a significant effect of ICV injection at 2 days (Fig 3C; LR $\chi2=7.26$, $p=0.027$, partial $\eta^2 = 0.277$) with *vVA* injected birds having higher *LHβ* mRNA expression compared to CV birds ($t=2.64$, $p=0.022$, Cohen's $d = 0.283$) indicating that *vVA* increased *LHβ* expression. There was no difference between CV and *vOPN5* birds ($t=0.72$, $p=0.487$, Cohen's $d = 0.100$). Chronic silencing had no effect on *LHβ* expression (Fig 3D LR $\chi2=2.56$, $p=0.279$, partial $\eta^2 = -4.11$). *vVA* and *vOPN5* groups did not show a significant reduction in *FSHβ* expression at 2 days LD (Fig 3E; LR $\chi2=5.45$, $p=0.066$, partial $\eta^2 = 0.999$). No effect of injection on *FSHβ* expression was detected following 7 days (LR $\chi2 = 1.47$, $p = 0.481$, partial $\eta^2 = 0.951$) nor 28 days (Fig 3F; LR $\chi2=2.16$, $p=0.339$, partial $\eta^2 = 0.785$) of photostimulation.

There was no effect of ICV injection nor a significant interaction when *TSHβ* expression was modelled over the entirety of the SD, 2 LD and 7 LD period. Due to the significant variation at 2 days, treatment days were analyzed separately. Based on Cook's distance analysis of the initial *TSHβ* glm model (at 2 days) residuals a single data point was identified as an outlier

441 (2.503 for bird 1703 CV at 2 days) and removed. Re-running of the analysis indicated that both
442 *vVA* and *vOPN5* significantly increased *TSHβ* expression at 2 days (Fig 3G; LR χ^2=16.81,
443 p<0.001, partial η^2 = 0.614). Post hoc testing indicated a very weak effect of *vOPN5* (t_{12}=2.19,
444 p=0.050, Cohen's d = 0.02) and a moderate effect of *vVA* (t_{12}=4.35, p<0.001, Cohen's d = 0.571)
445 silencing, increasing *TSHβ* expression compared to controls. No effect of injection was detected
446 at either 7 LD (LR χ^2=1.08, p=0.584, partial η^2 = 0.619) nor following 28 LD (Fig 3H; LR
447 χ^2=1.51, p=0.469, partial η^2 = 0.455).
448

449 # Discussion

450 We found that selective inhibition of VA opsin mRNA expression facilitated the
451 photoinduced increase of *TSHβ* and *LHβ* mRNA expression in quail. By 7 days, *GnRH-I* mRNA
452 levels and testes mass increased in *vVA* treated birds compared to controls. Birds treated with
453 shRNAi against OPN5 were only observed to show increased *TSHβ* expression during early
454 photostimulation (2 days). Silencing treatment inhibited both VA and OPN5 opsin expression
455 and reduced associated protein levels with the exception of a transient increase in VA opsin at 2
456 days of photostimulation. Overall, these represent the first causal evidence that VA opsin plays a
457 functional role in the light-dependent neuroendocrine control of seasonal reproduction in birds.
458 However, contrary to our a priori hypotheses, silencing of deep brain photoreceptors enhances
459 the response of the reproductive axis to photostimulation rather than preventing it. This
460 challenges our previous understanding of the functional role of deep brain photoreceptors in the
461 activation of the reproductive axis (Fig 4).
462

This study provides the first long-term functional investigation of the hypothalamic photoreceptors underpinning seasonal reproduction in birds. Previous studies have focused on the well-characterized first LD release model to examine the impact of short-term inhibition of OPN5 on photoinduced changes in *TSHβ* expression (Nakane et al., 2014; Stevenson and Ball, 2012), but have not explored long-term changes in neuroendocrine gene expression. In this study, long-term inhibition of VA and OPN5 was achieved using adeno-associated viral constructs (Nectow and Nestler, 2020). Using shRNAi, we are able to overcome the limitations and potential detrimental impacts associated with use of systemic genetic knockouts (also not currently available in quail) or lesions. By targeting both the early (i.e. 2-7 days) and late stages (i.e. 28 days) of photostimulation our study aimed to monitor photoperiod induced changes at genetic, physiological and morphological levels across time. Our findings expand our understanding of the mechanisms regulating the avian photoperiodic response, identifying the long-term impacts of VA and OPN5 inhibition on the neuroendocrine circuit that governs testicular growth and function. However, as the complex differential response of the various elements of the neuroendocrine cascade to silencing observed here highlights, transduction of photic cues is a multi-modal process relying on multiple receptor types and likely multiple receptor populations (Stevenson et al., 2022). These features make it challenging to isolate the full role of even a single photoreceptor type in detail.

VA as a multi-modal photoreceptor for the avian photoperiodic response

Our findings identified that *vVA* significantly increased both TSHβ and LHβ at 2 LD. Subsequently, GnRH-I and paired testes mass were increased at 7 LD. Interestingly, VA opsin is

487 closely related to the visual opsins phylogenetically (Beaudry et al., 2017; Soni et al., 1998);
488 both are within the subfamily of photoreceptors that activate intracellular Gα proteins by
489 catalyzing the exchange of GDP to GTP (Shichida and Matsuyama, 2009). Activation of
490 photoreceptors that couple the Gt subtype (i.e. rods, VA) generally decrease intracellular cGMP.
491 The second-messenger intracellular enzyme cyclic guanosine monophosphate (cGMP) has been
492 shown to bind to a 1.5kb enhancer motif upstream of the *GnRH-I* promoter repressing
493 transcription (Belsham et al., 1996). One potential link between light detection by VA opsin and
494 *GnRH-I* expression is via the direct action of cGMP and associated intracellular signaling
495 pathways. Immunohistochemical studies have demonstrated co-localization of VA and GnRH-I
496 in GnRH-I expressing neurons, in the anterior regions of the hypothalamus (García-Fernández et
497 al., 2015; Halford et al., 2009). Thus, we would expect tonic repression of *GnRH-I* expression in
498 these neurons that is released upon activation of VA opsin, based on the general mechanism of
499 action for opsin proteins. How then is it that silencing of the releaser, VA opsin, results in
500 upregulation of *TSHβ* and *LHβ mRNA* expression after 2 LD and particularly increased *GnRH-I*
501 expression and paired testes mass at 7 LD? The answer likely lies in the pathways that link VA
502 opsin to cGMP and *GnRH-I* transcription, and also the broad distribution of VA opsin within the
503 hypothalamus, where it has been identified in multiple nuclei (García-Fernández et al., 2015;
504 Halford et al., 2009). Co-expression of GnRH-I and VA opsin is limited primarily to anterior
505 nuclei: nucleus magnocellularis preopticus, nucleus anterior medialis hypothalamic, and the
506 nucleus supraopticus. Previous neuroanatomical analyses in European starling established that
507 the rostral preoptic area as the primary location of photoperiodic and gonadal hormone feedback
508 regulation on GnRH-I expression (Stevenson et al., 2009). However, there is also substantial VA
509 expression in the nucleus paraventricularis magnocellularis (both pars ventralis and medialis;

PVN) and the medial bed nucleus of stria terminalis with VA-ir positive fibers projecting into the median eminence with an apparent interface with the PT (Halford et al., 2009). These two VA opsin populations have the potential to independently regulate GnRH neuronal function and GnRH-I release. Our ICV injections were targeted to the 3V in the medial basal hypothalamus to optimize targeting of the PVN and ME, which contain both VA and OPN5 expression. Given the targeting of our injections, the spread of GFP expression and the fact we still detected some level of VA protein expression (Fig. 1) in our hypothalamic extracts, we posit that we were far more effective at silencing MBH expression than anterior hypothalamic expression of VA opsin. Based on this supposition and the anatomical localization of GnRH-I and VA opsin describe above we suggest that VA acts in a modular manner to regulate different aspects of GnRH-dependent control of reproductive physiology.

VA opsin neurons in the MBH project fibers through the ME to the PT allowing for direct interaction with PT based thyrotrophs. Silencing of VA expression in these cells results in the premature activation of these thyrotrophs resulting in the observed increase in *TSHβ* expression at 2D. Work in sheep has suggested anterograde signaling from the PT directly to the pars distalis of the anterior pituitary with respect to seasonal regulation of prolactin (Lincoln, 2002). Anterograde signaling from the PT to pars distalis gonadotrophs provides a plausible mechanism for the observed 2D elevation of *LHβ* in the vVA group. This model suggests some sort of inhibition of PT thyrotrophs by this population of VA neurons that is released by removing the opsin, likely requiring interaction with endogenous timing mechanisms. This population of VA neurons is anatomically positioned to provide indirect regulation of the reproductive axis via the canonical PT TSHβ to DIO2 pathway, potentially regulating GnRH release via modulation of tanycyte endfeet interaction with the GnRH-I nerve terminal (Yamamura et al., 2004). At present

533 there is no clear mechanism by which this would occur in VA expressing neurons, but the
534 proposed model provides a framework to further investigate the molecular and microcircuit
535 mechanisms involved.

536 Conversely, the second major population of VA expressing neurons in the anterior
537 portion of the hypothalamus appears to be the GnRH-I neurons themselves, opening the potential
538 for direct regulation of GnRH-I by VA opsin. Based of our GFP localization data we suggest that
539 this population of VA opsin experienced reduced silencing and potentially remained functionally
540 intact. Thus, photostimulation of VA opsin expression in these neurons is expected to have the
541 effect of increasing GnRH-I expression by reducing cGMP as described above. Taken together
542 with the above findings a timeline of VA activity can be formulated, suggesting that the
543 photoinducible phase involves a VA -dependent increase in *TSHβ* and the subsequent stimulation
544 of *LHβ* within 2 days of LD transfer mediated by the MBH populations of VA opsin expressing
545 neurons. Simultaneously, VA opsin expressed in GnRH-I neurons modulates GnRH-I expression
546 to support sustained release of GnRH-I triggered by the TSHβ induced conformational changes
547 in ventricular tanycytes. The enhancement of reproductive physiology induced by VA silencing,
548 supported by prolonged suppression of VA mRNA, suggests that MBH VA expressing cells may
549 be acting as a brake upon an otherwise active reproductive system, preventing its activation.
550 Under this model LD exposure results in the removal of inhibitory tone on pars tuberalis
551 thyrotrphs beginning the neuroendocrine cascade events leading to reproduction. However,
552 despite the consistent and reliable reduction in VA mRNA for several weeks we observed a
553 transient increase in VA opsin protein on day 2 of photostimulation (Fig. 1F). Increased VA
554 opsin protein may have resulted in a larger pool of receptors in the MBH to detect light at day 2.
555 Therefore our results may be alternatively explained by stimulatory activation of VA opsin cells

in the MBH early in the photoperiodic response that facilitated gonadal growth. However, under this explanation we might expect a subsequent decrease in gonadal growth later in photostimulation when VA opsin protein levels were reduced, which we do not see. Overall, the data reported herein provides the first functional evidence that VA opsin is integral to the photoperiodic response in birds. The precise mechanisms linking VA opsin to gonadotrophin release remain to be resolved, though it is clear that VA opsin influences GnRH-I mediated regulation of reproductive physiology on the scale of days to weeks.

.

OPN5 as a mediator of the initial photoperiodic response

The findings presented here also support a functional role for OPN5 in the initial light-dependent activation of seasonal reproduction. The current experimental design sought to identify the effects of OPN5 inhibition on pituitary secretagogue (i.e. *LHβ*, *FSHβ*) expression, identified as occurring early on the second LD in quail (Meddle and Follett, 1997). Early morning tissue collection limits comparisons with previous studies, which utilized later evening collections (Nakane et al., 2014; Stevenson and Ball, 2012). However, *TSHβ* expression was increased after 2 LD in *vOPN5* treated birds. These data are similar to reports from Border canaries in which shRNAi against OPN5 resulted in higher *TSHβ* expression 14 hours after light onset on the first LD (Stevenson and Ball, 2012). Interestingly, in the present study we do not find a clear long-term effect of *vOPN5* treatment on the HPG axis, suggesting that light activation of this photoreceptor has only a short-term effect on the photoperiodic response

limited to the first days following LD stimulation. Collectively, these data suggest that activation of OPN5 expressing cells is likely critical for early light detection and initiation of short-term effects on the avian photoperiodic response, but that longer term effects are dependent on input from other photoreceptors such as VA opsin.

Hierarchical organization of light detection by avian deep brain photoreceptors

In the quail hypothalamus, VA mRNA and protein expression is 2x and 20x higher than OPN5 respectively. In addition VA cells are identified in several nuclei and have immunoreactive fibers extend into multiple hypothalamic regions, in addition to the median eminence (Halford et al., 2009). The observed robust and long-term effects of *vVA* on multiple neuroendocrine substrates presented here suggest a predominant role for VA in the avian photoperiodic response, though whether via stimulatory pathways of removal of inhibitory tone remains to be confirmed. Furthermore, the VA action spectrum has the closest match to the action spectrum for the quail photoperiodic response and is the only photoreceptor to meet all the criteria set forth for the avian photoperiod response (García-Fernández et al., 2015). Therefore, we propose that light detection by VA expressing cells in the MBH is the primary mechanism for acute (1st week LD) photoinduction of reproductive physiology. However, it is likely that other photoreceptors, such as anterior hypothalamic VA opsin, OPN5 or perhaps even OPN4 provide additional input to facilitate the activation of the HPG axis.

A synthesis of the present and past studies highlights the complexity of opsin regulation of seasonal reproduction (Pérez et al., 2019). Combining our data with this past synthesis we propose a model of seasonal photoreception in which OPN5 expressing ependymal cells and

603 MBH VA cells regulate the initial response to photostimulation during the first long day by
604 acting on *TSHβ* expressing cells in the pars tuberalis to increase *TSHβ* expression (Nakane et al.,
605 2014; Stevenson and Ball, 2012). Simultaneously, VA expressing neurons in the preoptic
606 area/mediobasal hypothalamus respond to light stimulation over several days to weeks,
607 stimulating an increase in GnRH-I expression necessary to support long term activation of the
608 reproductive axis (Fig 4). Under this paradigm, VA serves as a long-term regulator, maintaining
609 the response to light and leading ultimately to reproductive competence. Whether these pathways
610 act completely independently or interact either directly, or indirectly, remains unclear at present.
611 Further work is needed to test the model proposed above and determine whether the involvement
612 of multiple opsins represents evolutionary redundancy or is a mechanism for enabling increased
613 flexibility and control of reproductive timing.
614
615

616 Acknowledgements

617 The authors would like to acknowledge Sir Brian Follet for his input and advice on the initial
618 development of this project and associated funding proposals.
619

620 References

621 Arnold, J.B., 2017. ggthemes: Extra themes, scales and geoms for '"ggplot2."'R package version
622 3.4. 0.
623 Baylé, J., Ramade, F., Oliver, J., 1974. Stereotaxic topogrphy of the brain of the quail (Coturnix
624 coturnix japonica). J. Physiol. 68, 219–241.

625 Beaudry, F.E.G., Iwanicki, T.W., Mariluz, B.R.Z., Darnet, S., Brinkmann, H., Schneider, P.,
626 Taylor, J.S., 2017. The non-visual opsins: eighteen in the ancestor of vertebrates,
627 astonishing increase in ray-finned fish, and loss in amniotes. J. Exp. Zool. Part B Mol. Dev.
628 Evol. 328, 685–696. https://doi.org/10.1002/jez.b.22773
629 Belsham, D.D., Wetsel, W.C., Mellon, P.L., 1996. NMDA and nitric oxide act through the
630 cGMP signal transduction pathway to repress hypothalamic gonadotropin-releasing
631 hormone gene expression. EMBO J. 15, 538–547.
632 Benoit, J., Ott, L., 1944. External and Internal Factors in Sexual Activity 17.
633 Chaurasia, S.S., Rollag, M.D., Jiang, G., Hayes, W.P., Haque, R., Natesan, A., Zatz, M., Tosini,
634 G., Liu, C., Korf, H.W., Iuvone, P.M., Provencio, I., 2005. Molecular cloning, localization
635 and circadian expression of chicken melanopsin (Opn4): Differential regulation of
636 expression in pineal and retinal cell types. J. Neurochem. 92, 158–170.
637 https://doi.org/10.1111/j.1471-4159.2004.02874.x
638 Davies, W.I.L., Turton, M., Peirson, S.N., Follett, B.K., Halford, S., Garcia-Fernandez, J.M.,
639 Sharp, P.J., Hankins, M.W., Foster, R.G., 2012. Vertebrate ancient opsin photopigment
640 spectra and the avian photoperiodic response. Biol. Lett. 8, 291–294.
641 https://doi.org/10.1098/rsbl.2011.0864
642 Dawson, A., King, V.M., Bentley, G.E., Ball, G.F., 2001. Photoperiodic control of seasonality in
643 birds. J. Biol. Rhythms 16, 365–380. https://doi.org/10.1177/074873001129002079
644 Follett, B.K., Pearce-Kelly, A.S., 1991. Photoperiodic induction in quail as a function of the
645 period of the light-dark cycle: implications for models of time measurement. J. Biol.
646 Rhythms 6, 331–341.
647 Follett, B.K., Sharp, P.J., 1969. Circadian rhythmicity in photoperiodically induced

gonadotrophin release and gonadal growth in the quail. Nature 223, 968–971.
Foster, R.G., Follett, B.K., 1985. The involvement of a rhodopsin-like photopigment in the photoperiodic response of the Japanese quail. J. Comp. Physiol. A 157, 519–528. https://doi.org/10.1007/BF00615153
Foster, R.G., Follett, B.K., Lythgoe, J.N., 1985. Rhodopsin-like sensitivity of extra-retinal photoreceptors mediating the photoperiodic response in quail. Nature 313, 50–52. https://doi.org/10.1038/313050a0
Foster, R.G., Hughes, S., Peirson, S.N., 2020. Circadian Photoentrainment in Mice and Humans. Biology (Basel). 9, 180.
Fox, J., Weisberg, S., 2019. An R Companion to Applied Regression, Third Edit. ed. Sage.
García-Fernández, J.M., Cernuda-Cernuda, R., Davies, W.I.L., Rodgers, J., Turton, M., Peirson, S.N., Follett, B.K., Halford, S., Hughes, S., Hankins, M.W., Foster, R.G., 2015. The hypothalamic photoreceptors regulating seasonal reproduction in birds: A prime role for VA opsin. Front. Neuroendocrinol. 37, 13–28. https://doi.org/10.1016/j.yfrne.2014.11.001
Halford, S., Pires, S.S., Turton, M., Zheng, L., González-Menéndez, I., Davies, W.L., Peirson, S.N., García-Fernández, J.M., Hankins, M.W., Foster, R.G., 2009. VA Opsin-Based Photoreceptors in the Hypothalamus of Birds. Curr. Biol. 19, 1396–1402. https://doi.org/10.1016/j.cub.2009.06.066
Hankins, M.W., Peirson, S.N., Foster, R.G., 2008. Melanopsin: an exciting photopigment. Trends Neurosci. 31, 27–36.
Kang, S.W., Leclerc, B., Kosonsiriluk, S., Mauro, L.J., Iwasawa, A., El Halawani, M.E., 2010. Melanopsin expression in dopamine-melatonin neurons of the premammillary nucleus of the hypothalamus and seasonal reproduction in birds. Neuroscience 170, 200–213.

https://doi.org/10.1016/j.neuroscience.2010.06.082

Kassambara, A., 2019. ggpubr:“ggplot2” based publication ready plots. R package version 3.4.0.

Lenth, R., Singmann, H., Love, J., Buerkner, P., Herve, M., 2018. Emmeans: Estimated marginal means, aka least-squares means. R Packag. version 1, 3.

Lincoln, G.A., 2002. Neuroendocrine regulation of seasonal gonadotrophin and prolactin rhythms: lessons from the Soay ram model. Reprod. Suppl. 59, 131–147.

MacDougall-Shackleton, S.A., Stevenson, T.J., Watts, H.E., Pereyra, M.E., Hahn, T.P., 2009. The evolution of photoperiod response systems and seasonal GnRH plasticity in birds. Integr. Comp. Biol. 49, 580–589.

Majumdar, G., Yadav, G., Rani, S., Kumar, V., 2014. A photoperiodic molecular response in migratory redheaded bunting exposed to a single long day. Gen. Comp. Endocrinol. 204, 104–113. https://doi.org/10.1016/j.ygcen.2014.04.013

Meddle, S.L., Follett, B.K., 1997. Photoperiodically Driven Changes in Fos Expression within the Basal Tuberal Hypothalamus and Median Eminence of Japanese Quail.

Meddle, S.L., Follett, B.K., 1995. Photoperiodic activation of Fos-like immunoreactive protein in neurones within the tuberal hypothalamus of Japanese quail. J. Comp. Physiol. A 176, 79–89. https://doi.org/10.1007/BF00197754

Menaker, M., Keatts, H., 1968. Extraretinal Light Perception In The Sparrow, II. Photoperiodic Stimulation of Testis Growth*. Proc. Natl. Acad. Sci. 60, 146–151. https://doi.org/10.1073/pnas.60.1.146

Menaker, M., Roberts, R., Elliott, J., Underwood, H., 1970. Extraretinal Light Perception in the Sparrow, III: The Eyes Do Not Participate in Photoperiodic Photoreception*.

Murrell, P., 2005. R Graphics. Chapman & Hall/CRC Press.

694 Nakane, Y., Ikegami, K., Ono, H., Yamamoto, N., Yoshida, S., Hirunagi, K., Ebihara, S., Kubo,
695 Y., Yoshimura, T., 2010. A mammalian neural tissue opsin (Opsin 5) is a deep brain
696 photoreceptor in birds. Proc. Natl. Acad. Sci. U. S. A. 107, 15264–15268.
697 https://doi.org/10.1073/pnas.1006393107
698 Nakane, Y., Shimmura, T., Abe, H., Yoshimura, T., 2014. Intrinsic photosensitivity of a deep
699 brain photoreceptor. Curr. Biol. 24, R596–R597. https://doi.org/10.1016/j.cub.2014.05.038
700 Nakane, Y., Shinomiya, A., Ota, W., Ikegami, K., Shimmura, T., Higashi, S.I., Kamei, Y.,
701 Yoshimura, T., 2019. Action spectrum for photoperiodic control of thyroid-stimulating
702 hormone in Japanese quail (Coturnix japonica). PLoS One 14, 1–15.
703 https://doi.org/10.1371/journal.pone.0222106
704 Nakao, N., Ono, H., Yamamura, T., Anraku, T., Takagi, T., Higashi, K., Yasuo, S., Katou, Y.,
705 Kageyama, S., Uno, Y., Kasukawa, T., Iigo, M., Sharp, P.J., Iwasawa, A., Suzuki, Y.,
706 Sugano, S., Niimi, T., Mizutani, M., Namikawa, T., Ebihara, S., Ueda, H.R., Yoshimura, T.,
707 2008. Thyrotrophin in the pars tuberalis triggers photoperiodic response. Nature 452, 317–
708 322. https://doi.org/10.1038/nature06738
709 Nectow, A.R., Nestler, E.J., 2020. Viral tools for neuroscience. Nat. Rev. Neurosci. 21, 669–681.
710 Oliver, J., Baylé, J.D., 1975. Multiple Unit Activity Patterns of Neuronal Populations in
711 Gonadotropic Areas of the Quail Hypothalamus: Spontaneous and Photically-Induced
712 Firing. Neuroendocrinology 17, 175–188. https://doi.org/10.1159/000122353
713 Peirson, S., Foster, R.G., 2006. Melanopsin: another way of signaling light. Neuron 49, 331–339.
714 Pérez, J.H., Swanson, R.E., Lau, H.J., Cheah, J., Bishop, V.R., Snell, K.R.S., Reid, A.M.A.,
715 Meddle, S.L., Wingfield, J.C., Krause, J.S., 2020. Tissue-specific expression of 11β-HSD
716 and its effects on plasma corticosterone during the stress response. J. Exp. Biol. 223.

https://doi.org/10.1242/jeb.209346

Pérez, J.H., Tolla, E., Dunn, I.C., Meddle, S.L., Stevenson, T.J., 2019. A Comparative Perspective on Extra-retinal Photoreception. Trends Endocrinol. Metab. 30, 39–53. https://doi.org/10.1016/j.tem.2018.10.005

Rowan, W., 1925. Relation of light to bird migration and developmental changes [3]. Nature 115, 494–495. https://doi.org/10.1038/115494b0

Shichida, Y., Matsuyama, T., 2009. Evolution of opsins and phototransduction. Philos. Trans. R. Soc. B Biol. Sci. 364, 2881–2895. https://doi.org/10.1098/rstb.2009.0051

Soni, B.G., Philp, A.R., Foster, R.G., Knox, B.E., 1998. Novel retinal photoreceptors [3]. Nature 394, 27–28. https://doi.org/10.1038/27794

Stevenson, T.J., Ball, G.F., 2012. Disruption of neuropsin mRNA expression via RNA interference facilitates the photoinduced increase in thyrotropin-stimulating subunit β in birds. Eur. J. Neurosci. 36, 2859–2865. https://doi.org/10.1111/j.1460-9568.2012.08209.x

Stevenson, T.J., Bernard, D.J., Ball, G.F., 2009. Photoperiodic condition is associated with region-specific expression of GNRH1 mRNA in the preoptic area of the male starling (Sturnus vulgaris). Biol. Reprod. 81, 674–680. https://doi.org/10.1095/BIOLREPROD.109.076794

Stevenson, T.J., Hahn, T.P., Macdougall-Shackleton, S.A., Ball, G.F., 2012. Gonadotropin-releasing hormone plasticity: A comparative perspective. Front. Neuroendocrinol. 33, 287–300. https://doi.org/10.1016/j.yfrne.2012.09.001

Stevenson, T.J., Liddle, T.A., Stewart, C., Marshall, C.J., Majumdar, G., 2022. Neural programming of seasonal physiology in birds and mammals: A modular perspective. Horm. Behav. 142. https://doi.org/10.1016/j.yhbeh.2022.105153

Wickham, H., Averick, M., Bryan, J., Chang, W., McGowan, L.D., François, R., Grolemund, G., Hayes, A., Henry, L., Hester, J., 2019. Welcome to the Tidyverse. J. Open Source Softw. 4, 1686.

Yamamura, T., Hirunagi, K., Ebihara, S., Yoshimura, T., 2004. Seasonal Morphological Changes in the Neuro-Glial Interaction between Gonadotropin-Releasing Hormone Nerve Terminals and Glial Endfeet in Japanese Quail. Endocrinology 145, 4264–4267. https://doi.org/10.1210/en.2004-0366

Statements and Declarations

Funding

This work was supported by: The Leverhulme Trust [RPG-2016-392] to TJS, SLM and ICD, Roslin Institute Strategic grant funding from the Biotechnology and Biological Sciences Research Council, UK (BB/P013759/1) to SLM and ICD and The British Society for Neuroendocrinology to JHP.

Competing Interests

The authors have no relevant competing financial or non-financial interests to disclose.

Author Contributions

TJS, SLM, ICD and RGF conceived of the initial study design. TJS, SLM and ICD secured and provided the grant funding for the experiments described. JHP, TJS, SLM and ICD refined initial experimental design. JHP carried out the experiments with SLM. JHP conducted all morphometric data collection. JHP, ET, VRB, and TJS conducted the molecular lab work. TJS and SNP designed the shRNAi sequences. RGF provided initial antibody stocks. JHP conducted the statistical analysis and drafted the main manuscript. All authors contributed to revision and editing of the draft manuscript prior to final submission

Data Availability

Data and analytic code (text format) for R analyses are provided in the supplementary files. For the purpose of open access, the author has applied a CC BY public copyright license to any Author Accepted Manuscript version arising from this submission.

Ethics Approvals

Animal procedures were approved by the Roslin Institute Animal Ethics and Welfare Review Board at the University of Edinburgh and were performed under Home Office approval (PPL P61FA9171). The experiments were designed in accordance with the Animal Research Reporting of In Vivo Experiments (ARRIVE) guidelines and National Centre for the Replacement, Refinement and Reduction of Animals in Research.

Figures

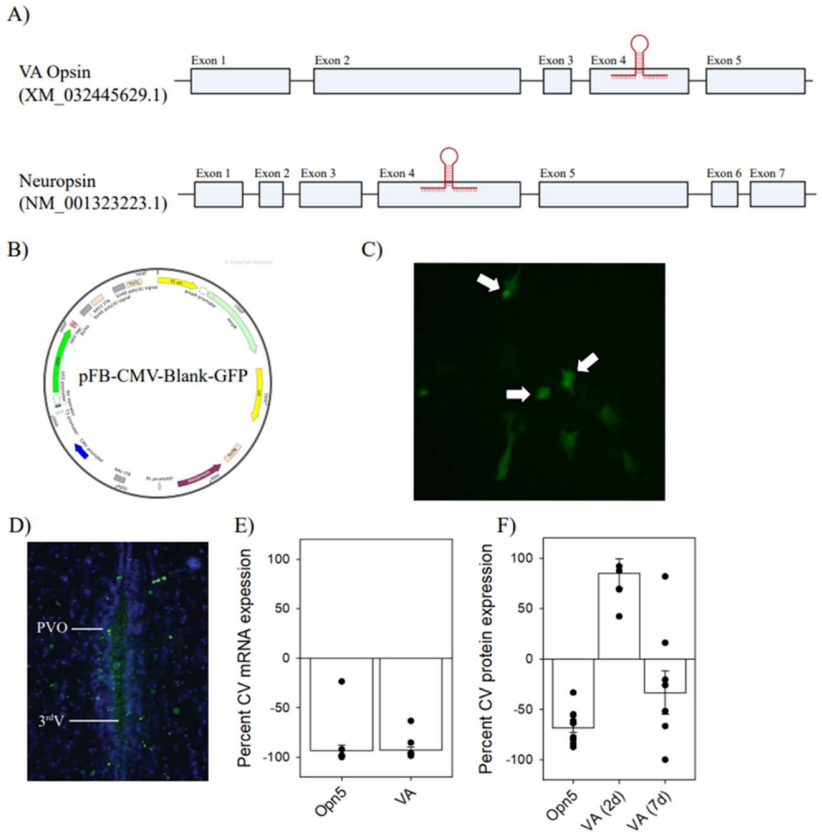

Fig. 1. Specificity and effectiveness of photoreceptor RNA interference

Specificity of RNA interference (RNAi) was achieved by designing probes that target Exon 4 in both VA opsin and Neuropsin (OPN5) sequences (A). Plasmids included a CMV promoter and green fluorescent protein (GFP). shRNAi vectors for VA opsin or OPN5 were inserted upstream to the CMV promoter, blank 'control' plasmid is shown (B). Primary cell culture of embryonic Japanese quail (E10) cells were used to confirm transduction capacity of AAV2 viral serotypes. Cells cultured with 2ul of AAV2 blank constructs showed robust transfection indicated by the white arrows (C). Representative photomicrograph of a coronal section through the mediobasal hypothalamus with the Periventricular organ (PVO) showing strong fluorescence. GFP expression was used to confirm the anatomical localization of intracerebroventricular injection of shRNAi constructs and presence of transfected cells 6-weeks after surgery (D). qPCR and western-blot assays were conducted to establish the effectiveness of shRNAi to reduced mRNA (E) and protein (F) expression for OPN5 and VA opsin. OPN5 mRNA and protein showed highly-effective reduction in photoreceptor expression. shRNAi against VA opsin induced a near 100% reduction in expression. VA opsin protein levels are shown separately for 2 day and 7-day treatment groups to highlight the variation across conditions. Higher VA opsin protein levels observed in 2-day birds likely reflects increased translation of VA opsin mRNA reserves or a transient disruption in the homeostatic balance of photoreceptor levels.

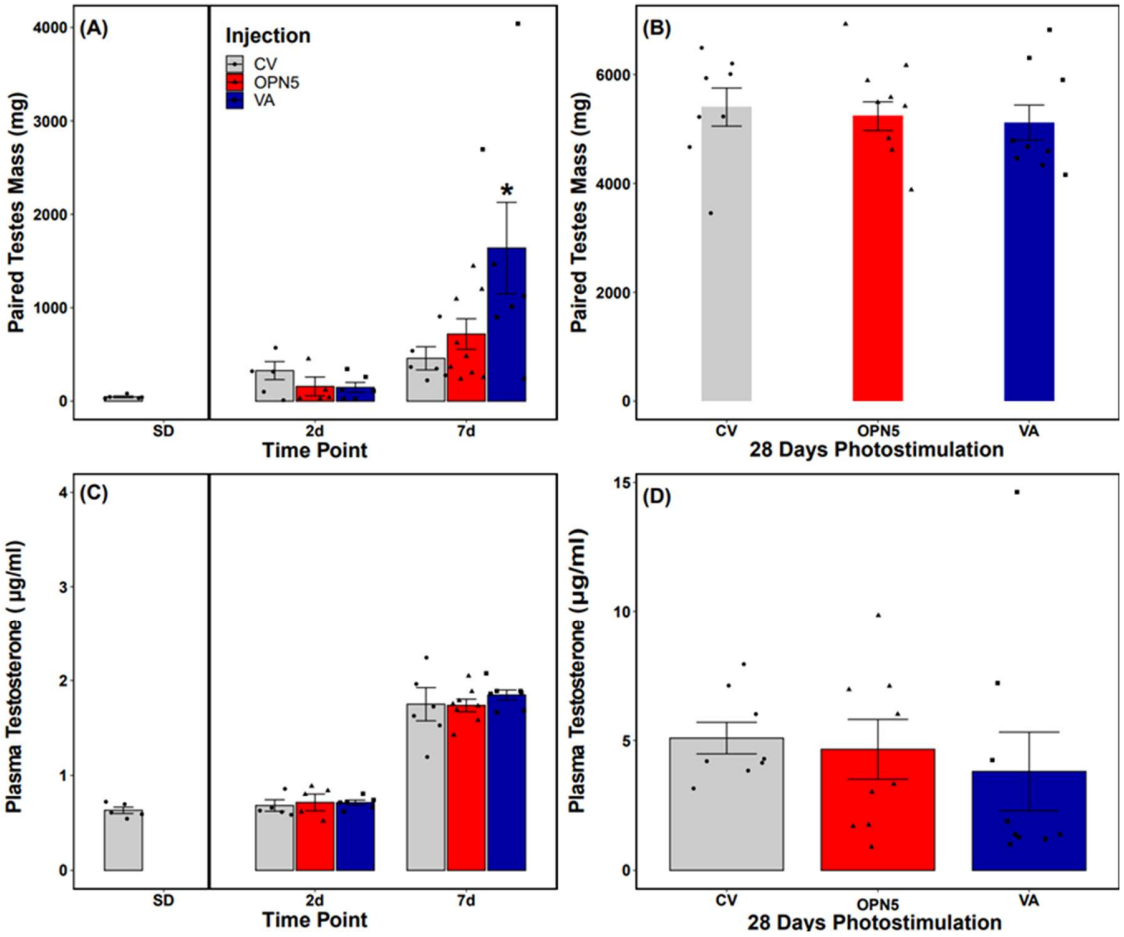

Fig 2. Effects of acute and chronic opsin silencing on opsin expression.

Effects of acute (A) or 28-day chronic (B) shRNAi knockdown of vertebrate ancient opsin (VA) and neuropsin (OPN5) compared to control AAV2 vector cassette (CV) on paired testes mass in Japanese quail reveals VA knockdown leads to accelerated induction of testes growth after 7 days of photostimulation (16L:8D). Plasma testosterone, (µg/ml) measured by ELISA, was unaffected by either acute (C) or 28-day chronic (D) opsin silencing, but increased with duration of photostimulation from acute to chronic. Asterisk (*) indicate $p < 0.05$ significant differences from control birds within the given time point. All values plotted as mean $\pm$ sem.

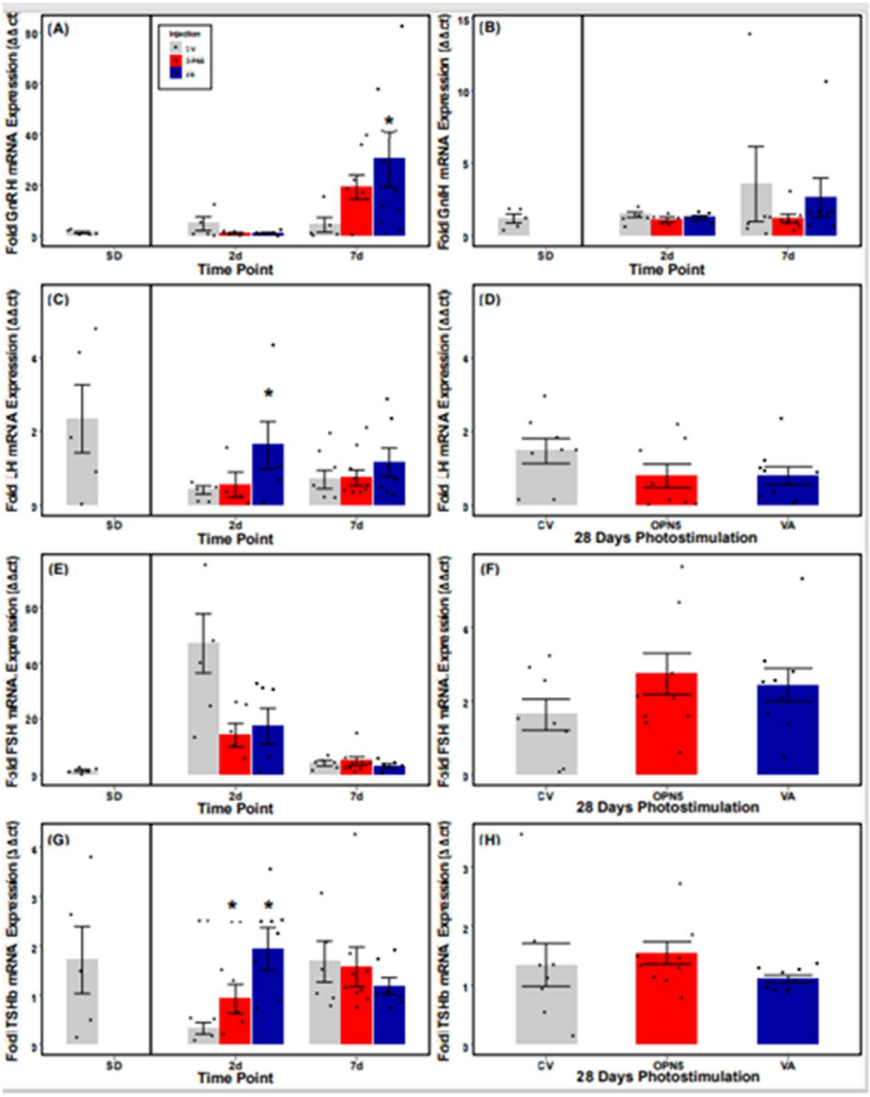

Fig 3. Photoinduced neuroendocrine gene expression.

Gene expression measured by RT-qPCR in control (CV) and vertebrate ancient opsin (VA) and neuropsin (OPN5) silenced quail for GnRH-I (A), GnIH (B), acute LH (C), 28-day chronic LH (D), acute FSH (E), 28-day chronic (F), acute TSHβ (G) and 28-day chronic TSHβ (H). Knockdown treatment induced increased TSHβ expression during the early photoinducible phase (2D) in both OPN5 and VA silenced animals, but only VA opsin knockdown effected gonadotroph expression with increased LH expression at 2 days and subsequently increased GnRH-I expression at 7 days of photostimulation. Asterisk (*) indicate $p < 0.05$ significant differences from control birds within the given time point. All values plotted as mean $\pm$ sem. Removed outliers are shown as black points, except in panel C where an outlier, value 10.52, in the CV at 2 days was removed.

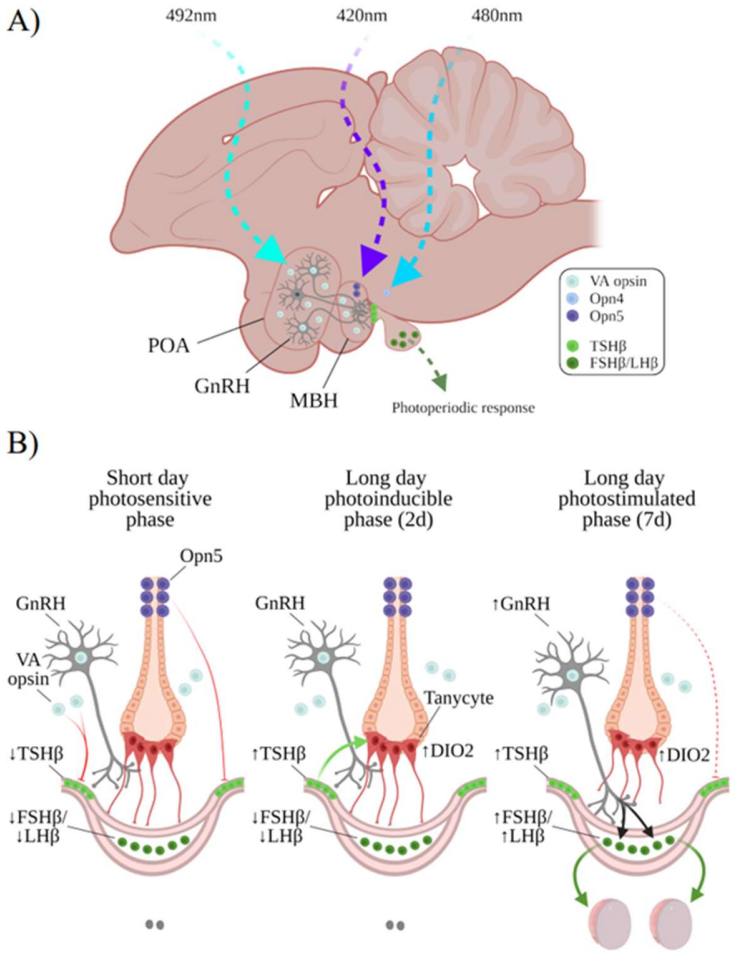

Fig 4. Schematic representation of the photoperiodic control of the neuroendocrine axis in birds. (A) Multiple wavelengths of light penetrate deep into the quail brain and are detected by at least three photoreceptors: vertebrate ancient opsin (VA opsin; λ492), neuropsin (OPN5; λ420) and melanopsin (OPN4; λ480). VA opsin is widely distributed in the preoptic area (POA) and mediobasal hypothalamus (MBH). OPN5 is localized to the PVO in the MBH and OPN4 is sparsely distributed in the MBH. Gonadotropin-releasing hormone (GnRH-I) neurons project from the preoptic area into the MBH to stimulate the release of luteinizing hormone (LH) and follicle-stimulating hormone (FSH). (B) Short day birds maintain regressed gonads due to an inability of GnRH-I neurons to contact the basal lamina membrane that separates the median eminence from the pituitary gland. Photoinduction by long days activates VA opsin and OPN5 cells located in the POA and mediobasal hypothalamus. Two- days light stimulation of VA opsin and OPN5 facilitated *TSHβ* expression. After 7 days of photostimulation of VA opsin either directly co-expressed in GnRH-I neurons or indirectly (via disinhibition from VA neurons) resulted in higher *GnRH* expression. GnRH-I access to the basal lamina permits that ability to stimulate gonadotropin release from the pituitary and trigger gonadal growth.

Supporting information

S1 Figure. 28 LD Testes histology and gene expression measured by qPCR. Gene expression metrics include Androgen Receptor (A), LH Receptor (B), and FSH Receptor (C). All gene expression values presented as fold expression using ΔΔCT method as describe in main text with GAPDH and β-Actin reference genes. Testes histology for Sox9 as a Sertoli cell marker (D), total number of tubules (E), and Sox9 positive cell to tubule ratio (F). For each testes marker treatment effect was analyzed by linear model. Line with "*" indicates a significant difference between treatment and control group $p < 0.05$.

S1 Table. AAV2 shRNA sequences used to suppress neuropsin and VA opsin expression

S2 Table. qPCR primers used for Japanese quail hypothalamus and annealing temperatures.

S3 Table. Antibody target and sequence for immunohistochemistry and western blot

S2 File. R analytic code and data file. The R code used for all analyses and figures presented in main and supporting documents as well as raw data file used in the analysis presented in a PDF format.